

A Study of the New Perovskite Solid Solution Series $\text{SrFe}_x\text{Ru}_{1-x}\text{O}_{3-y}$ by Ruthenium-99 and Iron-57 Mössbauer Spectroscopy

TERENCE C. GIBB, ROBERT GREATREX,
NORMAN N. GREENWOOD,* AND KENNETH G. SNOWDON

*Department of Inorganic and Structural Chemistry, The University of Leeds,
Leeds LS2 9JT, England*

Received July 1, 1974

The magnetic and structural properties of the solid solution $\text{SrFe}_x\text{Ru}_{1-x}\text{O}_{3-y}$ ($0 \leq x \leq 0.5$) have been studied using ^{57}Fe and ^{99}Ru Mössbauer spectroscopy and other techniques. These phases, which are here reported for the first time, have a distorted perovskite structure. The iron substitutes exclusively as Fe^{3+} and thereby causes oxygen deficiency, but has little effect on the magnetic behaviour of the Ru^{4+} until $x > 0.2$, whereupon the metallic band system begins to revert to a localized electron structure. The properties of a sample with $x = 0.3$ are complex and intermediate in character. For $x > 0.3$ the oxygen deficiency is reduced by substantial oxidation to Ru^{5+} until at $x = 0.5$ the system corresponds to $\text{Sr}_2\text{Fe}^{3+}\text{Ru}^{5+}\text{O}_6$.

Introduction

The ^{99}Ru Mössbauer spectra of solid solutions derived from the ferromagnetic perovskite SrRuO_3 (e.g., $\text{SrIr}_x\text{Ru}_{1-x}\text{O}_3$, $\text{SrMn}_x\text{Ru}_{1-x}\text{O}_3$ and $\text{Ca}_x\text{Sr}_{1-x}\text{RuO}_3$) have revealed much new information about the magnetic interactions in these systems and in the parent compound (1-3). In continuation of these studies it seemed particularly interesting to examine the phase $\text{SrFe}_x\text{Ru}_{1-x}\text{O}_{3-y}$, because SrFeO_3 is an antiferromagnetic Fe^{4+} perovskite and like SrRuO_3 is a metallic conductor. In this instance there is also the added advantage that it is possible to record Mössbauer spectra for both the transition metals in the phase. This paper reports the results of this investigation for $0 \leq x \leq 0.5$, which reveal some complex and unexpected features. Phases with $x > 0.5$ can also be prepared but were not studied in detail.

* Author to whom correspondence should be addressed.

Copyright © 1975 by Academic Press, Inc.
All rights of reproduction in any form reserved.
Printed in Great Britain

Experimental

Compounds in the series $\text{SrFe}_x\text{Ru}_{1-x}\text{O}_{3-y}$ with $x = 0.1, 0.2, 0.3, 0.4,$ and 0.5 were prepared from finely ground mixtures of strontium carbonate, ruthenium metal, and iron(III) oxide in stoichiometric proportions by heating in air, initially at 800°C for 3 hr to decompose the SrCO_3 and finally at 1100°C for 24 hr. SrRuO_3 was prepared by heating strontium carbonate and ruthenium metal in air at 1100°C using a published method (4). The resulting materials were examined with a Philips powder diffractometer using CuK_α radiation ($\lambda = 154.18$ pm), and were characterized as single phases with the perovskite lattice. Cell dimensions were derived from a least-squares refinement of the d -values.

The ferromagnetic phases of SrRuO_3 and $\text{SrFe}_{0.3}\text{Ru}_{0.7}\text{O}_{3-y}$ were studied using a vibrating sample magnetometer. The magnetic susceptibilities of all the phases were examined in the temperature range 85 - 300 K using a variable temperature Gouy balance. The

electrical resistivity was measured on compacted powder samples at room temperature.

The ^{57}Fe Mössbauer spectra for the iron-containing phases were measured at 300, 77 and 4.2 K using standard methods, and the ^{99}Ru Mössbauer spectra were recorded at 4.2 K using techniques described previously (3).

Crystallographic Data

The X-ray powder diffraction patterns of all the samples studied can be indexed as single-phase perovskite materials. Those for $x = 0, 0.1, 0.2$ and 0.3 were indexed on the basis of a distorted orthorhombic unit cell. Accurate indexing was not possible for $x = 0.4$ and 0.5 because the distortion was smaller and the lines were not resolved. The variation of unit cell dimensions is shown in Table I. Substitution of iron up to $x = 0.2$ causes a regular reduction in the cell volume. No reflections from a supercell were detected in any of the phases studied, and therefore a random distribution of the iron has been assumed. It will be shown later that for $x < 0.3$ the iron is present exclusively as the +3 oxidation state and ruthenium as the +4 oxidation state so that substitution by iron must lead to substantial oxygen deficiency. This increasing deficiency appears to dominate over the competing increase in the ionic radius of the cation, and results in the small decrease in cell volume observed.

It has not proved possible to measure the oxygen deficiency by direct chemical analysis. These inert refractory materials resist attack by normal analytical reagents, and the small percentage by weight of oxygen requires a minimum precision of analysis of $\pm 0.05\%$.

TABLE I
LATTICE PARAMETERS FOR THE PEROVSKITE PHASES
 $\text{SrFe}_x\text{Ru}_{1-x}\text{O}_{3-y}$

Phase	a/pm	b/pm	c/pm
SrRuO_{3-y}	552.6	556.4	784.2
$\text{SrFe}_{0.1}\text{Ru}_{0.9}\text{O}_{3-y}$	552.5	556.1	783.4
$\text{SrFe}_{0.2}\text{Ru}_{0.8}\text{O}_{3-y}$	552.5	555.8	782.8
$\text{SrFe}_{0.3}\text{Ru}_{0.7}\text{O}_{3-y}$	552.7	556.2	782.4

Hydrogen reduction, thermogravimetric analysis, X-ray fluorescence, and fast neutron activation analysis are some of the methods which we have tried in the search for a solution to the problem, but reproducible results with the required precision have not yet been achieved.

Electrical Resistivity

The electrical resistivity (ρ) of compacted powder samples at room temperature are as follows:

x	0.0	0.3	0.4	0.5
$\rho/(\text{ohm cm})$	0.00141	0.0224	0.138	153

These values are likely to be somewhat higher than single-crystal data; for example measurements on single crystals of SrRuO_3 (i.e., $x = 0$) have given a value of 2.7×10^{-4} ohm cm at 300 K (5). However, the results show clearly that increasing substitution of Fe^{3+} into SrRuO_3 causes an increase in resistivity. The metallic conduction in SrRuO_3 appears to be largely maintained up to $x = 0.3$, but the resistivity for $x = 0.5$ is more typical of a semiconductor and localized electron behaviour. The overlap of metal d -orbitals of t_{2g} symmetry with oxygen p_π orbitals leads to the formation of a metallic conduction band in SrRuO_3 and SrFeO_3 . The introduction of oxygen vacancies as Fe^{3+} is substituted for Ru^{4+} weakens the superexchange and causes a narrowing of the conduction band. Similar effects are seen in the SrFeO_{3-y} phase (6) where the increase in oxygen vacancies is paralleled by a decrease in the Néel temperature and an increase in resistivity as the superexchange interactions are weakened.

Magnetic Susceptibility

The end members of the phase are magnetically very different. SrRuO_3 is ferromagnetically ordered below $T_C = 160$ K (7), whereas SrFeO_3 is antiferromagnetically ordered below $T_N = 130$ K (6), with a spiral spin arrangement in the magnetic sublattices (8). For SrRuO_3 , which nominally has two unpaired $4d$ electrons, the low effective magnetic moment of $0.85 \mu_B$ at 77 K in a field of 1.0 T (7) is also consistent with a canted-spin arrangement, although

positive proof is not available (see discussion in Ref. (3)).

The magnetic susceptibility was measured in the temperature range 85–300 K for samples with $x = 0, 0.1, 0.2, 0.3, 0.4$ and 0.5 , and the results are shown in Fig. 1. Substitution of up to 20% Fe^{3+} for Ru^{4+} produces little change in the paramagnetic behaviour, except to lower the Curie temperature by ca. 16 K. The paramagnetic susceptibility for 30% substitution is significantly higher at 300 K, indicating a ferrimagnetic contribution. At lower temperatures the behaviour was closer to that of SrRuO_3 and the Curie temperature by extrapolation was ca. 134 K.

The phase with $x = 0.5$ is significantly different again, and the susceptibility follows the Curie–Weiss law with a negative Weiss constant of -344 K. This is typical of the anti-ferromagnetic interactions in the oxygen deficient strontium ferrates.

Because the phase $\text{SrFe}_{0.3}\text{Ru}_{0.7}\text{O}_{3-y}$ is significantly different from the end-members of the series, the ferromagnetic phase was studied down to 4.2 K using a vibrating sample magnetometer. The spontaneous ferromagnetic moment in zero applied field is shown as a function of temperature in Fig. 2 with comparative data for SrRuO_3 . The solid line is the $S = 1$ Brillouin function appropriate

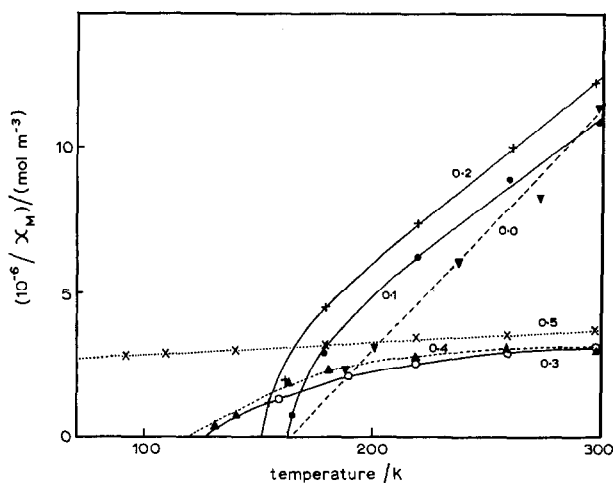


FIG. 1. The temperature dependence of the reciprocal susceptibility ($1/\chi_M$) for five samples of the phase $\text{SrFe}_x\text{Ru}_{1-x}\text{O}_{3-y}$. The values of x are indicated.

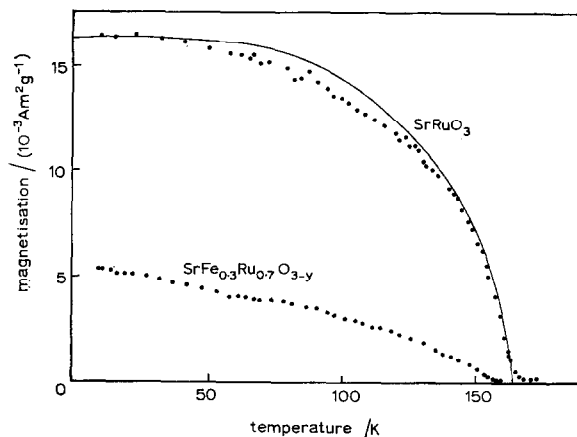


FIG. 2. The temperature dependence of the spontaneous magnetization in SrRuO_3 and $\text{SrFe}_{0.3}\text{Ru}_{0.7}\text{O}_{3-y}$.

to the $4d^4$ low-spin configuration. The spontaneous moment for $x = 0.3$ is much smaller than that of SrRuO_3 , being approximately 25% of this magnitude. There is also a small residual parasitic ferromagnetism in the region of 160–170 K which persists to higher temperatures and is the probable cause of the anomalously high paramagnetic susceptibility recorded using the Gouy balance.

The X-ray data showed no other phases, and a ^{57}Fe Mössbauer spectrum recorded at 300 K for 14 days showed no evidence of long-range magnetic order, thereby eliminating many of the possible iron-bearing impurities. This parasitic ferromagnetism is therefore believed to be a characteristic of the phase, and not due to impurities. Such behaviour is not uncommon in mixed perovskite phases, and is known in the nonstoichiometric strontium ferrates (9).

The parasitic moment was estimated from an extrapolation of the linear plot of observed magnetization σ at 300 K against applied field strength H using the relationship

$$\sigma = \sigma_0 + \chi H$$

where σ_0 is the parasitic contribution and χ is the paramagnetic susceptibility. This led to a value for χ_M of $1.23 \times 10^{-7} \text{ m}^3 \text{ mole}^{-1}$ with $\theta = 150 \text{ K}$, and an effective moment of $3.43 \mu_B$. This compares favourably with a calculated value of $3.75 \mu_B$ (assuming spin-only values for high-spin Fe^{3+} and low-spin Ru^{4+}), and is clearly more realistic than the total observed value of $5.65 \mu_B$.

Mössbauer Measurements

The problem of oxygen deficiency is a major difficulty in the investigation of this phase, particularly when both the transition metals have alternative oxidation states. For this reason the ^{57}Fe and ^{99}Ru Mössbauer resonances have been obtained to define more clearly the relative proportions of Fe^{3+} , Fe^{4+} , Ru^{4+} , and Ru^{5+} which are present in each sample.

(A) ^{57}Fe Mössbauer Spectra

The Mössbauer resonance of Fe^{4+} in metallic perovskite systems is clearly distin-

guishable from that of Fe^{3+} . Thus, in SrFeO_3 the chemical isomer shift of Fe^{4+} is $+0.147 \text{ mm s}^{-1}$ at 4 K and $+0.055 \text{ mm s}^{-1}$ at 298 K relative to iron metal, compared to values of $+0.494 \text{ mm s}^{-1}$ at 4 K and $+0.352 \text{ mm s}^{-1}$ at 298 K, respectively, for octahedral-site Fe^{3+} in $\text{SrFeO}_{2.5}$ (10). Furthermore, the magnetic hyperfine splitting at Fe^{4+} in SrFeO_3 at 4 K is 33.1 T , compared to the much larger value of 53.8 T for Fe^{3+} in $\text{SrFeO}_{2.5}$. On this basis, the $\text{Fe}^{4+}/\text{Fe}^{3+}$ ratio should be easily determined from the relative areas of the different components in the spectrum, although lack of knowledge concerning the recoilless fractions may introduce some slight error.

The ^{57}Fe Mössbauer spectra at room temperature for $x = 0.1, 0.2, 0.3, 0.4$ and 0.5 are shown in Fig. 3, and the corresponding data at 78 K are shown in Fig. 4. Spectra for $x = 0.2, 0.3, 0.4$ and 0.5 were also obtained at 4.2 K, and that for $x = 0.3$ is shown in Fig. 5; this is typical of all four spectra and shows that long-range magnetic ordering of the iron is present. The single hyperfine pattern indicates a flux density of ca. 49.5 T , which is typical of Fe^{3+} in an octahedral site. No trace of a hyperfine pattern with a flux density of ca. 33 T was found. Values for the magnetic flux density B , the chemical isomer shift δ , and the average of the widths of the two outer lines Γ are given in Table II. The unusually large linewidth is indicative of the variation in nearest-neighbour environment being experienced by the Fe^{3+} ions, which results in a range in values of the magnetic flux density and the obscuration of any small quadrupole coupling.

The paramagnetic spectra at room temperature (Fig. 3) confirm the absence of Fe^{4+} , but reveal more clearly the presence of multiple Fe^{3+} environments, some of which feature quadrupole splitting. For $x = 0.1$ and 0.2 a simple model is proposed in which those Fe^{3+} sites with a neighbouring O^{2-} anion vacancy show a quadrupole splitting, while the remainder in a more nearly regular octahedral site contribute a single-line resonance. The relevant computed parameters are collected together in Table III. For $x = 0.3, 0.4$, and 0.5 the spectra approximate to a quadrupole doublet but with a broader linewidth and have

been fitted accordingly. In all cases the widths of the two components of the doublet were constrained to be equal, but the intensities were left unconstrained. As can be seen in Fig. 3, this interpretation is at best an approximation.

The quadrupole splitting value of ca. 0.50 mm s^{-1} for $x = 0.1$ and 0.2 is in good agreement with the value of 0.42 mm s^{-1} found in the oxygen deficient system $\text{Sr}_3\text{Fe}_2\text{O}_{6.2}$ (II). Both chemical isomer shifts are typical of Fe^{3+} in octahedral coordination in oxides. The relative area of the doublet increases rapidly as x and the number of vacancies increases. If

a formulation of $\text{SrFe}_x^{3+}\text{Ru}_{1-x}^{4+}\text{O}_{3-x/2}$ is adopted, then for $x = 0.1$ there are 1.66% oxygen sites vacant. If these vacancies are completely random, then 90% of the Fe^{3+} sites should have no immediate neighbouring vacancy, this figure decreasing to 81% at $x = 0.2$. The observed figures of 52 and 38%, respectively, imply a tendency for the Fe^{3+} site and the vacancy to be more frequently contiguous than is required by a truly random distribution.

It is noteworthy that the linewidth of the doublet is much larger for $x > 0.2$, and this

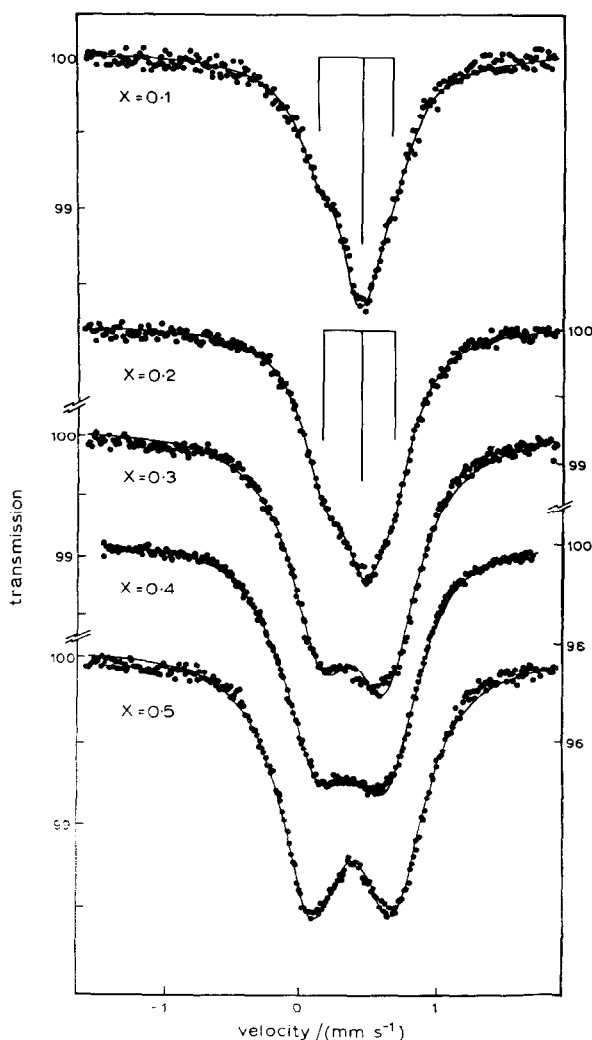


FIG. 3. ^{57}Fe Mössbauer spectra for $\text{SrFe}_x\text{Ru}_{1-x}\text{O}_{3-y}$ at room temperature. The solid lines indicate three- or two-line computed fits as appropriate, and in all cases the linewidths of the doublet were constrained to be equal.

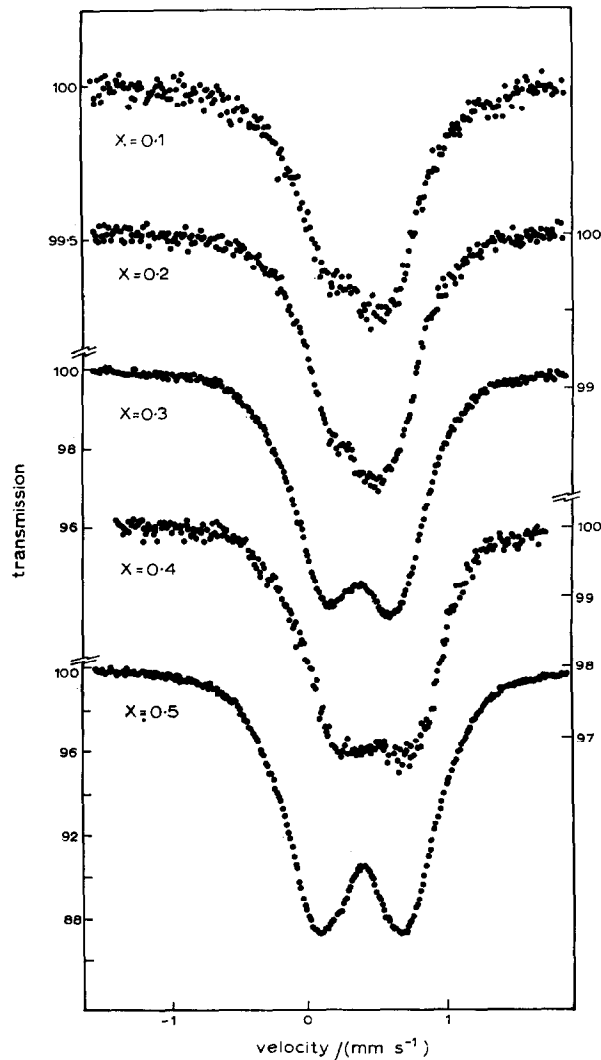


FIG. 4. ^{57}Fe Mössbauer spectra for $\text{SrFe}_x\text{Ru}_{1-x}\text{O}_{3-y}$, at 78 K with the source at the same temperature (except for $x = 0.4$ at 85 K; in this case the source was at room temperature, resulting in the apparent chemical isomer shift).

probably reflects a major structural change between $x = 0.2$ and 0.3 .

The ^{57}Fe spectra at 78 K are basically similar to the high-temperature spectra, and for $x > 0.2$ they are again significantly broader. Perhaps surprisingly, there is no obvious sign of magnetic order in the iron spectra despite the temperature being well below the Curie temperature of the phase, although for $x = 0.1$ in particular the overall spectrum envelope

appears more diffuse. A possible explanation is that the Fe^{3+} ions are magnetically dilute from each other and couple only weakly to Ru^{4+} [the $180^\circ t_{2g}^3 e_g^2 - t_{2g}^4$ interaction is not expected to be strong (12)] so that they have a short relaxation time close to the Curie temperature, and only show hyperfine splitting at low temperatures. It is ultimately hoped to examine the temperature dependence of the spectra below 78 K to verify this point.

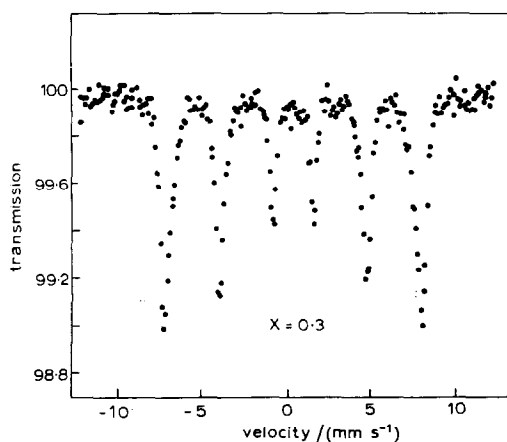


FIG. 5. ^{57}Fe Mössbauer spectrum at 4.2 K for $\text{SrFe}_{0.3}\text{Ru}_{0.7}\text{O}_{3-y}$.

TABLE II

^{57}Fe MÖSSBAUER PARAMETERS AT 4.2 K FOR $\text{SrFe}_x\text{Ru}_{1-x}\text{O}_{3-y}$

x	0.2	0.3	0.4	0.5
$\delta/(\text{mm s}^{-1})^a$	+0.45	+0.44	+0.42	+0.42
B/T	49.6	49.1	48.9	49.1
$\Gamma/(\text{mm s}^{-1})^b$	0.72	0.78	0.77	0.77
$\chi^2(d = 230)$	515	414	860	186

^a Measured with the source of $^{57}\text{Co}/\text{Rh}$ at 4.2 K; add 0.127 mm s^{-1} to convert to a source at room temperature.

^b Averaged value for the outer pair of lines only. The inner lines are proportionately narrower.

(B) ^{99}Ru Mössbauer Spectra

The ^{99}Ru Mössbauer spectra at 4.2 K of the samples with $x = 0.1$ and 0.2 are shown in Fig. 6, and for $x = 0.3, 0.4,$ and 0.5 (note the expanded velocity scale) in Fig. 7. The spectrum of the end-member SrRuO_3 has been illustrated and interpreted previously (1, 2) and comprises a complex spectrum of 18 overlapping lines associated with magnetic hyperfine splitting of the $I_g = 5/2 \rightarrow I_e = 3/2$

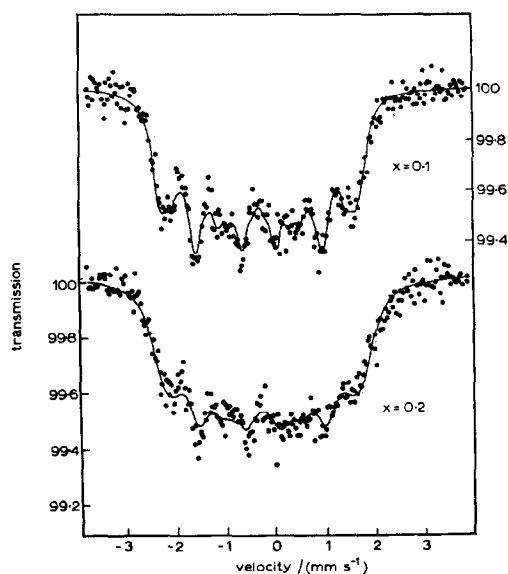


FIG. 6. ^{99}Ru Mössbauer spectra at 4.2 K for $\text{SrFe}_{0.1}\text{Ru}_{0.9}\text{O}_{3-y}$ and $\text{SrFe}_{0.2}\text{Ru}_{0.8}\text{O}_{3-y}$. The solid lines are appropriate to Model 2 and Model 4 in Table IV, respectively.

TABLE III

^{57}Fe MÖSSBAUER PARAMETERS AT ROOM TEMPERATURE FOR $\text{SrFe}_x\text{Ru}_{1-x}\text{O}_{3-y}$

x	0.1		0.2		0.3	0.4	0.5
$\Delta/(\text{mm s}^{-1})$	0.518	0	0.489	0	0.465	0.474	0.495
$\delta/(\text{mm s}^{-1})^a$	0.389	0.441	0.405	0.439	0.373	0.356	0.380
$\Gamma/(\text{mm s}^{-1})$	0.409	0.353	0.408	0.398	0.559	0.598	0.552
% area	48	52	62	38	—	—	—
$\chi^2(d = 245)$	372		323		615	1345	364

^a δ is the chemical isomer shift relative to iron metal. Approximate errors are $\pm 0.01 \text{ mm s}^{-1}$.

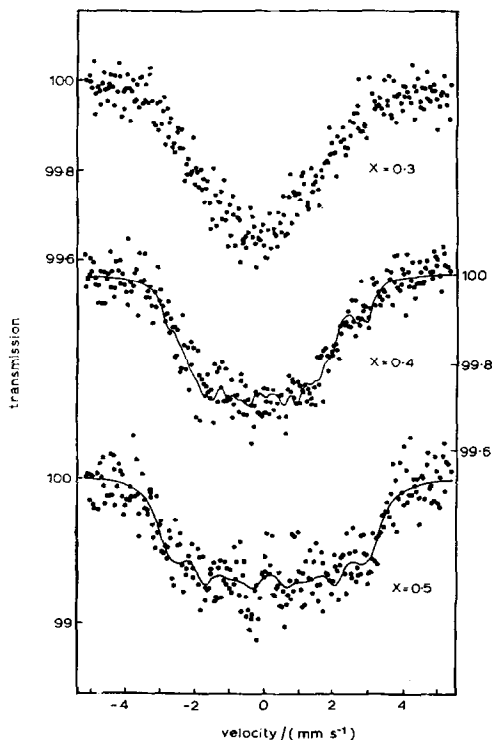


FIG. 7. ^{99}Ru Mössbauer spectra at 4.2 K for $\text{SrFe}_x\text{Ru}_{1-x}\text{O}_3$. The solid lines for $x = 0.4$ and $x = 0.5$ are appropriate to Model 2 and Model 1 in Table IV, respectively.

transition. In earlier measurement on the phase $\text{SrIr}_x\text{Ru}_{1-x}\text{O}_3$ it was found that the hyperfine field at the ruthenium decreased proportionally with the number of substituted cations in the first coordination sphere (2). Thus the magnetic flux density B in SrRuO_3 was reduced to $B - \Delta B$ for one substituent neighbour, to $B - 2\Delta B$ for two neighbours, etc., and the resultant spectrum was the weighted sum of the various hyperfine patterns. Similar behaviour has also been found in the phase $\text{Ca}_x\text{Sr}_{1-x}\text{RuO}_3$ where the divalent cation has a marked effect on the magnetic interactions (3). The net result is seen as an inward broadening and partial collapse of the spectrum.

In the present system, the spectra for $x = 0.1$ and 0.2 are unusual in being very similar to the spectrum of SrRuO_3 . The magnetic flux density at the Ru is apparently little affected by the substitution. Both sets of data have been computer-fitted using the methods given

in Ref. (2) and under the assumption that the magnetic flux density has a unique value. The results are given in Table IV. The spectrum for $x = 0.1$ proves to be particularly well defined, and the flux density of $35.7 T$ is only slightly larger than $35.2 T$ found in SrRuO_3 . For $x = 0.2$ the flux density is $36.2 T$, but the resonance lines are much broader, and constraining the linewidth to the value for $x = 0.1$ raises the value of χ^2 substantially. Both sets of data were also analysed using the multiple-field model, and with B fixed at $35.2 T$ gave values for ΔB of $+1.27 T$ and $+1.06 T$, respectively. This incremental flux density is to be compared to the values of $-6.0 T$ in $\text{SrIr}_x\text{Ru}_{1-x}\text{O}_3$ and $-2.2 T$ in $\text{SrMn}_x\text{Ru}_{1-x}\text{O}_3$.

The spectrum for $x = 0.5$ features very broad lines, but is otherwise consistent with a unique magnetic flux density of $52.9 T$; this is substantially higher than in SrRuO_3 and the low-iron content phases. The chemical isomer shift of $+0.116 \text{ mm s}^{-1}$ is also more positive than in any of the typical Ru^{4+} oxides, and is of the order of magnitude expected for Ru^{5+} . This oxidation state has a $4d^3$ configuration with $s = 3/2$ and is akin to Fe^{3+} in that the magnetic flux density should vary little with change in environment. The flux density of $52.9 T$ corresponds, therefore, to about $17.6 T$ per unpaired electron. On this basis, the flux density at Ru^{4+} with $S = 1$ should be $35.2 T$, which is in very good agreement with observation, and lends support to the belief that SrRuO_3 has a canted-spin structure, rather than a reduced-moment ferromagnetism occasioned by partial band overlap.

The spectrum for $x = 0.4$ is clearly the superposition of two hyperfine fields from Ru^{4+} and Ru^{5+} . The results of two computer fits with a variable and fixed linewidth, respectively, are given in Table IV. In both cases the magnetic flux densities are very similar to the values for $x = 0$ and $x = 0.5$, and confirm the assignment. The proportion of Ru^{5+} in the two instances is 35 and 48%, respectively.

The spectrum for $x = 0.3$ is inconsistent with the rest of the series. It is too diffuse to allow a multifield calculation, and contrasts with the more regular behaviour for $x = 0.2$

TABLE IV
 ^{99}Ru MÖSSBAUER PARAMETERS AT 4.2 K FOR $\text{SrFe}_x\text{Ru}_{1-x}\text{O}_{3-y}$

	Model	B/T	AB/T	$\Gamma/(\text{mm s}^{-1})$	$\delta/(\text{mm s}^{-1})$	$\chi^2 (d)$
$x = 0.1$						
(Single field)	1	35.7 (1)	—	0.310 (12)	-0.307 (5)	277 (247)
(Multifield)	2	35.2 ^a	+1.27 (21)	0.31 ^a	-0.311 (5)	271 (248)
$x = 0.2$						
(Single field)	1	36.2 (2)	—	0.517 (30)	-0.250 (10)	316 (246)
	2	35.8	—	0.31 ^a	-0.269 (6)	422 (247)
(Multifield)	3	32.8 (4)	+3.1 (4)	0.370 (37)	-0.248 (8)	303 (245)
	4	35.2 ^a	+1.06 (18)	0.50 (3)	-0.249 (10)	313 (246)
	5	35.2 ^a	+1.5 (2)	0.31 ^a	-0.249 (6)	397 (247)
$x = 0.4$						
	1	35.6 (1.5)	—	0.99 (23)	-0.219 (54)	294 (242)
		50.6 (3.3)	—	0.99 (23)	+0.188 (145)	
	2	34.9 (6)	—	0.41 ^a	-0.252 (25)	312 (243)
		51.2 (7)	—	0.41 ^a	+0.113 (24)	
$x = 0.5$						
(Single field)	1	52.9 (7)	—	0.74 (9)	+0.116 (38)	697 (244)

^a Fixed values. $\mu_e/\mu_g = 0.456$, $\delta^2 = 2.70$.

and 0.4. However, it seems to be compatible with the proposed change in structural characteristics in this region, and it probably corresponds to high oxygen deficiency, and an irregular spin structure caused by the conflicting requirements of ferromagnetic coupling between Ru and antiferromagnetic coupling between Fe. The centroid of the spectrum lies at about -0.27 mm s^{-1} which is still consistent with Ru^{4+} , but in view of the broadening of the spectrum wings it is possible that a small proportion of Ru^{5+} is also present.

Conclusions

The results of these various measurements can be summarized as follows. Substitution of Fe for Ru^{4+} in the perovskite SrRuO_3 takes place exclusively as Fe^{3+} . It has little effect on the magnetic and electronic properties of the system for values of x up to 0.2 despite the increasing oxygen deficiency, and the samples prepared appear to have compositions close to $\text{SrFe}_{0.1}^{3+}\text{Ru}_{0.9}^{4+}\square_{0.05}\text{O}_{2.95}$ and $\text{SrFe}_{0.2}^{3+}\text{Ru}_{0.8}^{4+}\square_{0.10}\text{O}_{2.90}$ where \square indicates an oxygen vacancy. These vacancies associate closely with the Fe^{3+} cations. Between $x = 0.2$ and

$x = 0.3$ an appreciable change in the structure is indicated by X-ray crystallography, the magnetic properties, and the Mössbauer spectra. The sample with $x = 0.3$ appears to be intermediate between a collective-electron and a localized-electron system, and the magnetic interactions are complex because of the competing exchange mechanisms. For $x > 0.3$ the band structure has totally collapsed, and there is an increasing proportion of Ru^{5+} until in the phase $\text{SrFe}_{0.5}^{3+}\text{Ru}_{0.5}^{5+}\text{O}_3$ the oxygen deficiency appears to be minimal. An approximate formulation for the sample with $x = 0.4$ is $\text{SrFe}_{0.4}^{3+}\text{Ru}_{0.39}^{4+}\text{Ru}_{0.21}^{5+}\square_{0.09}\text{O}_{2.91}$. It appears that, under the conditions of preparation, the perovskite system is unable to tolerate more than about 3–4% oxygen deficiency, and as a result, partial oxidation of Ru^{4+} to Ru^{5+} occurs, rather than the introduction of Fe^{4+} which might have been predicted.

Acknowledgments

We thank Dr. D. A. Read of the Department of Physics for the use of the vibrating sample magnetometer, Dr. D. C. Puxley for assistance with the X-ray powder diffraction work, and the Science Research Council for financial support and for a maintenance grant (to K.G.S.).

References

1. T. C. GIBB, R. GREATREX, N. N. GREENWOOD, AND P. KASPI, *Chem. Commun.* 319 (1971).
2. T. C. GIBB, R. GREATREX, N. N. GREENWOOD, AND P. KASPI, *J. Chem. Soc. (Dalton Trans.)*, 1253 (1973).
3. T. C. GIBB, R. GREATREX, N. N. GREENWOOD, D. C. PUXLEY, AND K. G. SNOWDON, *J. Solid State Chem.* **11**, 17 (1974).
4. J. J. RANDALL AND R. WARD, *J. Amer. Chem. Soc.* **81**, 2629 (1959).
5. R. J. BOUCHARD AND J. L. GILLSON, *Mat. Res. Bull.* **7**, 873 (1972).
6. J. B. MACCHESNEY, R. C. SHERWOOD, AND J. F. POTTER, *J. Chem. Phys.* **43**, 1907 (1965).
7. A. CALLAGHAN, C. W. MOELLER, AND R. WARD, *Inorg. Chem.* **5**, 1572 (1966).
8. T. TAKEDA, Y. YAMAGUCHI, AND H. WATANABE, *J. Phys. Soc. Japan* **33**, 967 (1972).
9. T. R. CLEVINGER, *J. Amer. Ceram. Soc.* **46**, 207 (1963).
10. P. K. GALLAGHER, J. B. MACCHESNEY, AND D. N. E. BUCHANAN, *J. Chem. Phys.* **41**, 2429 (1964).
11. P. K. GALLAGHER, J. B. MACCHESNEY, AND D. N. E. BUCHANAN, *J. Chem. Phys.* **45**, 2466 (1966).
12. J. B. GOODENOUGH, "Magnetism and the Chemical Bond," Interscience, New York, 1963.